

A Standard Siren Cosmological Measurement from the Potential GW190521 Electromagnetic Counterpart ZTF19abnrhr

Hsin-Yu Chen,^{1,2,3,*} Carl-Johan Haster,^{2,3,†} Salvatore Vitale,^{2,3,‡} Will M. Farr,^{4,5,§} and Maximiliano Isi^{2,3,¶}

¹*Black Hole Initiative, Harvard University, Cambridge, Massachusetts 02138, USA*

²*LIGO Laboratory, Massachusetts Institute of Technology, 185 Albany St, Cambridge, MA 02139, USA*

³*Department of Physics and Kavli Institute for Astrophysics and Space Research,*

Massachusetts Institute of Technology, 77 Massachusetts Ave, Cambridge, MA 02139, USA

⁴*Center for Computational Astrophysics, Flatiron Institute, 162 5th Ave, New York, NY 10010, USA*

⁵*Department of Physics and Astronomy, Stony Brook University, Stony Brook NY 11794, USA*

(Dated: September 30, 2020)

The identification of the electromagnetic counterpart candidate ZTF19abnrhr to the binary black hole merger GW190521 opens the possibility to infer cosmological parameters from this standard siren with a uniquely identified host galaxy. The distant merger allows for cosmological inference beyond the Hubble constant. Here we show that the three-dimensional spatial location of ZTF19abnrhr calculated from the electromagnetic data remains consistent with the latest sky localization of GW190521 provided by the LIGO-Virgo Collaboration. If ZTF19abnrhr is associated with the GW190521 merger, and assuming a flat w CDM model, we find that $H_0 = 48_{-10}^{+23} \text{ km s}^{-1} \text{ Mpc}^{-1}$, $\Omega_m = 0.35_{-0.26}^{+0.41}$, and $w_0 = -1.31_{-0.48}^{+0.61}$ (median and 68% credible interval). If we use the Hubble constant value inferred from another gravitational-wave event, GW170817, as a prior for our analysis, together with assumption of a flat Λ CDM and the model-independent constraint on the physical matter density ω_m from Planck, we find $H_0 = 68.9_{-6.0}^{+8.7} \text{ km s}^{-1} \text{ Mpc}^{-1}$.

INTRODUCTION

Gravitational waves (GWs) emitted by compact object binaries are self-calibrating standard sirens [1], in that they yield a direct measurement of the source luminosity distance. If the redshift of the source can be estimated by other means, then GWs provide a way to measure cosmological parameters that is entirely independent from classic probes such as those based on standard candles [2, 3], the cosmic microwave background (CMB) [4, 5] and other methods [6–9]. While a few different ways have been proposed to measure the redshift of the binary source, which is *not* encoded in the GW signal [10–13], the two most prominent are the identification of an electromagnetic (EM) counterpart, and a statistical analysis of all galaxies included in the GW uncertainty volume [1, 14–16]. To date, both approaches have been explored [17]. The detection of GWs from the binary neutron star (BNS) merger GW170817 [18] by the LIGO/Virgo Collaboration (LVC) [19, 20], together with the observation of EM counterparts at multiple wavelengths [21] has allowed the first-ever standard siren measurement of the Hubble constant [22]. While the statistical standard siren method has the advantage that it can be applied to all types of compact binary coalescences (CBCs), whether they emit light or not, it is intrinsically less precise, as usually many galaxies are consistent with the GW uncertainty volume [16, 17, 23].

The recent identification of an EM transient at non-negligible redshift ($z \simeq 0.4$) by the Zwicky Transient Facility (ZTF) — ZTF19abnrhr [24] — consistent with being a counterpart to the distant (~ 4 Gpc) binary black hole (BBH) GW source GW190521 [25–27] (see also [28]

for a new evaluation of the confidence), offers the potential to measure cosmological parameters beyond the Hubble constant using GW observations. If indeed a non-negligible fraction of BBHs merge in gas-rich environments such as the disks of active galactic nuclei (AGN) and emit observable EM signals [24, 29], they might contribute significantly to the cosmological inference from standard siren measurements [16]. Previous cosmological inference from GW observations has been limited to the local Hubble parameter H_0 , primarily due to the GW detectors’ current limit in their sensitive distance to BNSs, and the number of galaxies consistent with the large BBH uncertainty volumes. Inference on other cosmological parameters was expected to rely on future GW observations at higher redshift [13, 30–32]

ZTF19ABANRHR ASSOCIATION IN 3D LOCALIZATION

In Figure 1(a) we show the three-dimensional localization uncertainty volume of GW190521 assuming a flat prior in luminosity volume ($\propto D_L^3$). Using a Planck 2018 cosmology [5], we also mark the location of ZTF19abnrhr. We found that ZTF19abnrhr lies at a 67% credible level of the GW190521 localization volume.

The credible level at which the counterpart lies in the localization of GW190521 depends on the assumed prior distribution of GW sources. Figure 1(b) shows the posterior distribution of luminosity distance along the line of sight to ZTF19abnrhr for several different choices of prior; in all cases the luminosity distance to ZTF19abnrhr computed from a reasonable cosmol-

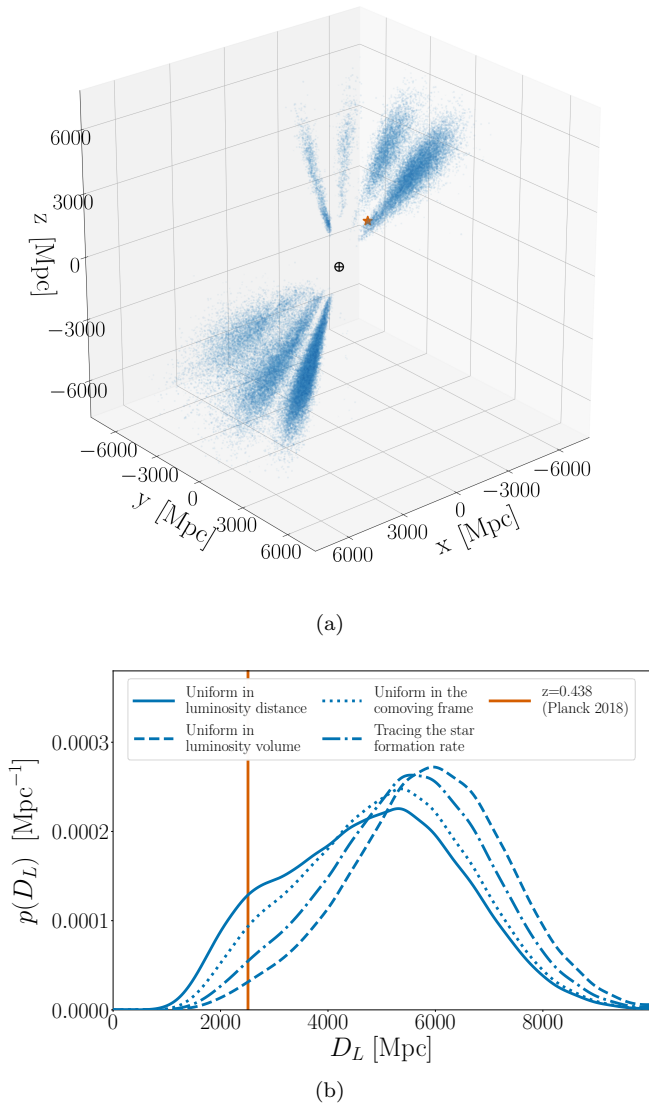


FIG. 1. Panel (a): The 3D localization of GW190521 presented in a Cartesian luminosity distance coordinates, centered on the Earth marked with a black \oplus . Here we use the localization inferred by the NRSur analysis from [27, 33] which applied a flat prior in luminosity volume. The size and hue of each point is weighted by the logarithm of its posterior probability. The location of ZTF19abahrh, assuming the Planck 2018 cosmology [5], is shown by the orange star. Panel (b): The 1D D_L posterior for GW190521 along the line of sight to ZTF19abahrh under four different prior assumptions for the luminosity distance D_L [34]. The location of ZTF19abahrh, assuming the Planck 2018 cosmology [5], is shown by the orange line. The priors are (solid blue line) uniform in luminosity distance (i.e. proportional to the conditional distance likelihood); uniform in luminosity volume (dashed blue line); uniform in the comoving frame (dotted blue line); and tracing the star formation rate [35] (dash-dotted blue line).

ogy [5] is found well within the bulk of this *conditional* distance distribution. For the primary estimate of the distance marginal used in this study, we rely on a parameter estimation analysis conditional on J1249 + 3449, the sky location of ZTF19abahrh [34, 36], and otherwise matching the preferred analysis from [27, 33, 37].

COSMOLOGICAL INFERENCE

The mathematical and statistical background behind a standard siren measurement of the Hubble constant has already been presented in the literature [1, 14, 16, 22, 38, 39]. In this letter, we follow the same framework to infer the Hubble constant H_0 , the matter density of the Universe Ω_m and the dark energy equation of state (EoS) parameter w_0 .

Given a set of GW data \mathcal{D}_{GW} and EM data \mathcal{D}_{EM} corresponding to a common observation, the joint posterior of (H_0, Ω_m, w_0) can be written as:

$$p(H_0, \Omega_m, w_0 | \mathcal{D}_{\text{GW}}, \mathcal{D}_{\text{EM}}) = \frac{p(H_0, \Omega_m, w_0)}{\beta(H_0, \Omega_m, w_0)} \times \int p(\mathcal{D}_{\text{GW}} | \vec{\Theta}) p(\mathcal{D}_{\text{EM}} | \vec{\Theta}) p_{\text{pop}}(\vec{\Theta} | H_0, \Omega_m, w_0) d\vec{\Theta}, \quad (1)$$

where $\vec{\Theta}$ represents all the binary parameters, such as the masses, spins, luminosity distance, sky location, orbital inclination etc. $p(H_0, \Omega_m, w_0)$ denotes the prior probability density function (PDF) on the cosmological parameters. $p_{\text{pop}}(\vec{\Theta} | H_0, \Omega_m, w_0)$ is the distribution of the population of binaries with parameters $\vec{\Theta}$ in the Universe. The denominator, β , is the *fraction* of the population of events that would pass detection thresholds [22, 38, 40–43]:

$$\beta(H_0, \Omega_m, w_0) \equiv \int P_{\text{det}}(\vec{\Theta}) p_{\text{pop}}(\vec{\Theta} | H_0, \Omega_m, w_0) d\vec{\Theta} \quad (2)$$

where

$$P_{\text{det}}(\vec{\Theta}) \equiv \iint_{\substack{\mathcal{D}_{\text{GW}} > \text{GW}_{\text{th}}, \\ \mathcal{D}_{\text{EM}} > \text{EM}_{\text{th}}}} p(\mathcal{D}_{\text{GW}} | \vec{\Theta}) p(\mathcal{D}_{\text{EM}} | \vec{\Theta}) d\mathcal{D}_{\text{GW}} d\mathcal{D}_{\text{EM}}, \quad (3)$$

is the probability of detecting a source with parameters $\vec{\Theta}$ in GW and EM emission. This latter integration should be carried out over data above the GW and EM detection thresholds, GW_{th} and EM_{th} . We assume that the counterparts to systems like GW190521 can be observed by ZTF and other telescopes far beyond the distance at which GW observatories can detect them (ZTF19abahrh was ~ 18.8 mag in g-band at $z=0.438$), so the integral's domain is truncated by GW selection effects.

To evaluate Eq. (1) we need to specify the distribution for the parameters of the underlying population of BBH mergers with counterparts, $p_{\text{pop}}(\vec{\Theta} | H_0, \Omega_m, w_0)$. Since

the astrophysical rate of GW190521-like BBHs is still uncertain, we assume their redshift distribution follows the star formation rate (SFR) as modeled by Ref. [35]. We adopt the default assumptions of [27] that the population is flat in the detector frame masses¹ and spin magnitudes and isotropic over binary and spin orientations.

Given the small uncertainty in the redshift and counterpart sky location measured in ZTF19abnrhr, we treat the EM likelihood in Eq. (1) as a δ -function at these measurements. Performing the integral over $\vec{\Theta}$, Eq. (1) becomes

$$p(H_0, \Omega_m, w_0 | \mathcal{D}_{\text{GW}}, \mathcal{D}_{\text{EM}}) \propto p(\mathcal{D}_{\text{GW}} | D_L(z_{\text{EM}} | H_0, \Omega_m, w_0), \alpha_{\text{EM}}, \delta_{\text{EM}}) \times \frac{p_{\text{pop}}(z_{\text{EM}} | H_0, \Omega_m, w_0)}{\beta(H_0, \Omega_m, w_0)} p(H_0, \Omega_m, w_0). \quad (4)$$

The first term is the marginalized GW likelihood evaluated at the right ascension α , declination δ , and luminosity distance implied by the redshift of ZTF19abnrhr given cosmological parameters H_0 , Ω_m and w_0 ; this function is shown by the solid blue curve in Figure 1(b). The next term accounts for selection effects and the assumed GW source population and involves the ratio of the (normalized) population density at the ZTF19abnrhr redshift and the fraction of the (normalized) population that is jointly detectable in GW and EM emission as described above (in the local universe the effect of this term is to introduce a factor $1/H_0^3$ [22, 38] but at $z \simeq 0.4$ cosmological effects weaken the dependence on H_0 substantially [44]). The third term is the prior on cosmological parameters. We impose several different priors incorporating various additional cosmological measurements in the following.

In our most generic analysis, we use flat priors in the ranges $H_0 = [35, 140] \text{ km s}^{-1} \text{ Mpc}^{-1}$, $\Omega_m = [0, 1]$, and $w_0 = [-2, -0.33]$. The result is presented in Fig. 2. We find a broad posterior for H_0 with a median and 68% credible interval of $H_0 = 48.3_{-10}^{+23} \text{ km s}^{-1} \text{ Mpc}^{-1}$, with a peak below the maximum likelihood Planck 2018 value [5] (as well as the SH0ES estimate [2]), reported with a yellow (pink) solid line. The Planck and SH0ES estimates are contained within the 90% credible regions of our measurements. The posteriors for Ω_m and w_0 are nearly uninformative with $\Omega_m = 0.35_{-0.26}^{+0.41}$, and $w_0 = -1.31_{-0.48}^{+0.61}$. Nevertheless, given the large inferred distance of GW190521, they are mildly correlated with H_0 , and must be included in the analysis.

A joint GW190521–ZTF19abnrhr analysis furnishes a single measurement of the luminosity distance to

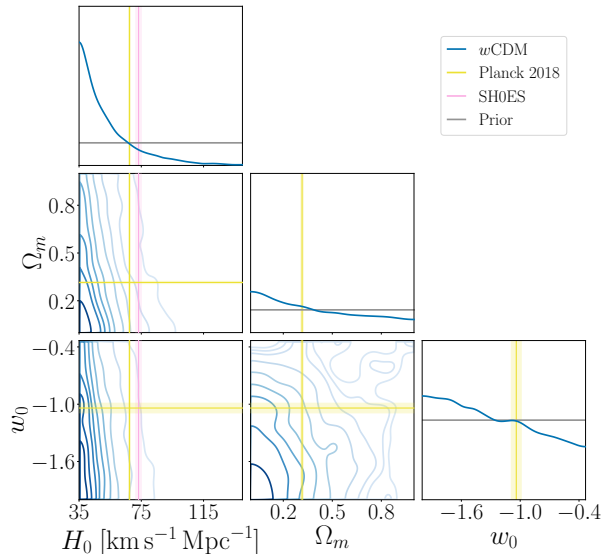


FIG. 2. The joint posterior PDF of H_0 , Ω_m and w_0 for the associated GW190521–ZTF19abnrhr observations using uniform priors (grey lines) for all parameters in a flat w CDM cosmology. The yellow (pink) solid lines report the Planck 2018 [5] (SH0ES [2]) cosmology, with shaded regions representing their respective 68% credible interval. For the 2D plots, the contours are spaced 10 percentiles apart, from the 10% (darkest) to 90% (lightest) credible regions.

ZTF19abnrhr, which depends on H_0 , Ω_m and w_0 . To compare with other GW measurements in the local universe, which depend only on H_0 , we restrict to Λ CDM universes ($w = -1$) and apply the model-independent measurement of the physical matter density [45] from Planck observations of the CMB [5], $\omega_m \equiv \Omega_m h^2 = 0.1428 \pm 0.0011$ as a prior. The result is shown in the light blue curve in Figure 3. We find $H_0 = 48.3_{-8.1}^{+21.5} \text{ km s}^{-1} \text{ Mpc}^{-1}$ with this assumption. The model-independence of the ω_m constraint means this measurement remains systematically independent of early-universe distance scales from CMB measurements.

The best inference on H_0 from gravitational wave standard sirens comes from combining our measurement here with GW170817. We apply the H_0 likelihood from GW170817 [17, 22] as a prior on H_0 along with the Planck ω_m constraint. These results are shown in the dark blue curve in Fig. 3. The joint measurement is narrower than either measurement alone, with a median and 68% credible interval of $H_0 = 68.9_{-6.0}^{+8.7} \text{ km s}^{-1} \text{ Mpc}^{-1}$ and a clear peak consistent with estimates using observations from both the CMB [5] and the local distance ladders [2, 3, 6–9]; GW190521 rules out some large H_0 values that are permitted from GW170817.

The choice of waveform models for GW data analy-

¹ The priors are uniform on the component masses in the detector frame from $[30, 200]M_\odot$. The mass priors are further restricted such that the total mass must be greater than $200M_\odot$, and the chirp mass to be between 70 and $150M_\odot$, both in the detector frame. The mass ratio between the lighter and heavier objects is restricted to be > 0.17 .

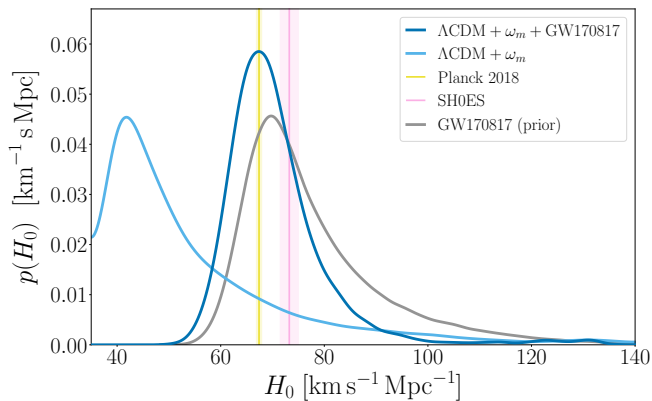


FIG. 3. The posterior PDF of H_0 for the associated GW190521–ZTF19abnr observations under the assumption of a flat Λ CDM cosmology and physical matter density ω_m constraints from Planck 2018 [5]. The dark blue curve uses the inferred H_0 posterior from GW170817 [17, 22] (grey curve) as a prior whereas the light blue curve assumes a flat prior on H_0 . The yellow (pink) solid lines report the Planck 2018 [5] (SH0ES [2]) H_0 estimates, with shaded regions representing their respective 68% credible interval.

sis can contribute to the systematic uncertainty of the standard siren measurement via the luminosity distance estimate. In Ref. [27], the LVC estimated the parameters of GW190521 with three different waveform models [37, 46, 47]. We use a clustering decomposition followed by a kernel density estimate within clusters [44] to estimate the marginal posterior probability distribution of D_L along the line-of-sight to ZTF19abnr [24] from these analyses. In Figure 4 we show the H_0 inference with the three waveform models using the GW170817 prior on H_0 and Planck’s prior on ω_m in a Λ CDM cosmology. The strong prior on H_0 dominates over the slight difference between D_L estimates from different models, and they all yield a very similar posterior on H_0 .

Finally, in Figure 5 we present the measurements on Ω_m and w_0 with both of the GW events and Planck’s prior on ω_m in a flat w CDM cosmology. We find that the Ω_m posterior now shows a departure from its prior, and features a peak with a median and 68% credible interval of $\Omega_m = 0.298^{+0.061}_{-0.064}$. To a lesser extent, the same is true for w_0 now estimated as $w_0 = -1.33^{+0.63}_{-0.47}$.

DISCUSSION

The EM transient ZTF19abnr [24] could be associated with the BBH merger GW190521. We find that ZTF19abnr lies at the 67% credible level of the GW190521 three-dimensional localization volume under a default luminosity-distance prior and assuming the Planck 2018 cosmology [5]. Assuming the GW–EM association is true, we report a standard-siren measurement

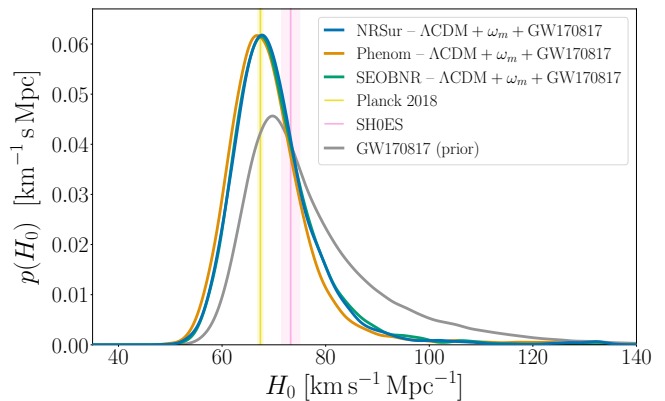


FIG. 4. The posterior PDF of H_0 for the associated GW190521–ZTF19abnr observations using ω_m constraints from Planck 2018 [5], a prior on H_0 from GW170817 [17, 22] (shown in grey) and a flat Λ CDM cosmology. We show estimates on H_0 using all three waveform analyses from Ref. [27, 33]. The yellow (pink) solid lines report the Planck 2018 [5] (SH0ES [2]) cosmology, with shaded regions representing their respective 68% credible interval.

of cosmological parameters from these transients. The large inferred distance of GW190521 enables probing H_0 and additional cosmological parameters Ω_m and the dark energy EoS parameter w_0 . We note that other independent analyses also conduct the standard-siren measurement assuming the association between GW190521 and ZTF19abnr [48, 49].

We find $H_0 = 68.9^{+8.7}_{-6.0} \text{ km s}^{-1} \text{ Mpc}^{-1}$ from the associated ZTF19abnr–GW190521 and the kilonova AT 2017gfo–GW170817 observations assuming a model-independent constraints on the physical matter density ω_m from the Planck observations [5] in a flat Λ CDM cosmology. The same measurement yields $\Omega_m = 0.298^{+0.061}_{-0.064}$ and $w_0 = -1.33^{+0.63}_{-0.47}$ in a flat w CDM cosmology. Since there is only one standard siren measurement at higher redshift, the inference on Ω_m mainly relies on the prior from GW170817 and Planck. The strong prior on H_0 from GW170817 dominates the H_0 measurement. When GW170817 is combined with the Planck prior on ω_m , Ω_m is constrained to $\sim 20\%$. On the other hand, without any informative priors, w_0 is only marginally confined even when both GW170817 and GW190521 are included in the analysis.

We find that the choice of GW waveform for the estimation of luminosity distance and the assumption of BBH population for the evaluation of selection effect do not introduce noticeable difference in our results. However, when more events are combined in the future and the cosmological parameters are confined more precisely, the systematic uncertainties arising from waveform and selection effect will have to be investigated more carefully. For example, a joint inference of the BBH population and the cosmological parameters will help reduce

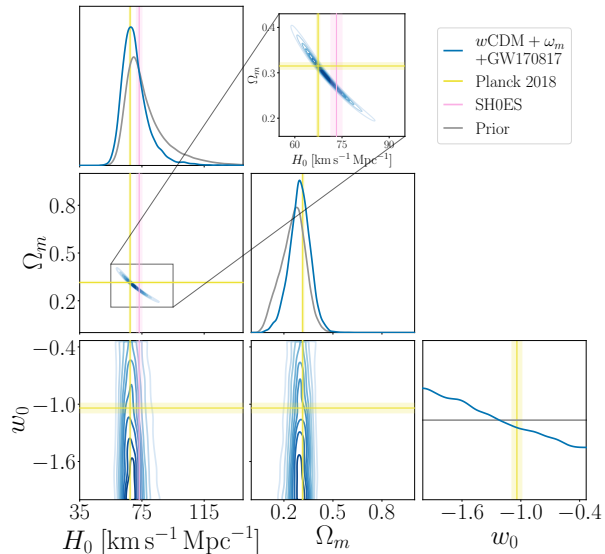


FIG. 5. The joint posterior PDF of H_0 , Ω_m and w_0 for the associated GW190521–ZTF19abarr observations using a prior for H_0 equal to the posterior of GW170817 [17, 22], and additional constraints on ω_m from Planck 2018 [5], shown as grey curves. The yellow (pink) solid lines report the Planck 2018 [5] (SH0ES [2]) cosmology, with shaded regions representing their respective 68% credible interval. For the 2D plots, the contours are spaced 10 percentiles apart, from the 10% (darkest) to 90% (lightest) credible regions.

bias from unrealistic population assumptions.

In the next five years, LIGO, Virgo and KAGRA are predicted to detect hundreds of BBHs per year [50]. If indeed ZTF19abarr is the counterpart of GW190521, we should see more BBHs accompanied by EM counterparts. Owing to their generally larger distances, compared to standard BNS bright sirens, these have a significant potential of yielding an interesting GW measurement of Ω_m and w_0 .

The authors would like to thank Jonathan Gair his review and suggestions to this work. HYC was supported by the Black Hole Initiative at Harvard University, which is funded by grants from the John Templeton Foundation and the Gordon and Betty Moore Foundation to Harvard University. HYC and MI are supported by NASA through NASA Hubble Fellowship grants No. HST-HF2-51452.001-A and No. HST-HF2-51410.001-A awarded by the Space Telescope Science Institute, which is operated by the Association of Universities for Research in Astronomy, Inc., for NASA, under contract NAS5-26555. CJH and SV acknowledge support of the National Science Foundation, and the LIGO Laboratory. LIGO was constructed by the California Institute of Technology and Massachusetts Institute of Technology with funding

from the National Science Foundation and operates under cooperative agreement PHY-1764464. This research has made use of data, software and/or web tools obtained from the Gravitational Wave Open Science Center (<https://www.gw-openscience.org>), a service of LIGO Laboratory, the LIGO Scientific Collaboration and the Virgo Collaboration. LIGO is funded by the U.S. National Science Foundation. Virgo is funded by the French Centre National de Recherche Scientifique (CNRS), the Italian Istituto Nazionale della Fisica Nucleare (INFN) and the Dutch Nikhef, with contributions by Polish and Hungarian institutes. This analysis was made possible by the numpy [51, 52], SciPy [53], matplotlib [54], emcee [55], pandas [56, 57], pymc3 [58], seaborn [59] and astropy [60, 61] software packages. This is LIGO Document Number LIGO-P2000233. The data behind Figures 1(b), 2, 3, 4 and 5 are publicly available at [62].

* himjiu@mit.edu; NHFP Einstein fellow

† haster@mit.edu

‡ salvatore.vitale@ligo.mit.edu

§ will.farr@stonybrook.edu

¶ maxisi@mit.edu; NHFP Einstein fellow

- [1] B. F. Schutz, *Nature* **323**, 310 (1986).
- [2] A. G. Riess et al., *Astrophys. J.* **826**, 56 (2016), 1604.01424.
- [3] A. G. Riess, S. Casertano, W. Yuan, L. M. Macri, and D. Scolnic, *Astrophys. J.* **876**, 85 (2019), 1903.07603.
- [4] P. Ade et al. (Planck), *Astron. Astrophys.* **594**, A13 (2016), 1502.01589.
- [5] N. Aghanim et al. (Planck), *Astron. Astrophys.* **641**, A6 (2020), 1807.06209.
- [6] E. Macaulay et al. (DES), *Mon. Not. Roy. Astron. Soc.* **486**, 2184 (2019), 1811.02376.
- [7] W. Yuan, A. G. Riess, L. M. Macri, S. Casertano, and D. Scolnic, *Astrophys. J.* **886**, 61 (2019), 1908.00993.
- [8] W. L. Freedman et al., *Astrophys. J.* **882**, 34 (2019), 1907.05922.
- [9] D. Pesce et al., *Astrophys. J. Lett.* **891**, L1 (2020), 2001.09213.
- [10] C. Messenger, K. Takami, S. Gossan, L. Rezzolla, and B. S. Sathyaprakash, *Phys. Rev. X* **4**, 041004 (2014), 1312.1862.
- [11] W. M. Farr, M. Fishbach, J. Ye, and D. Holz, *Astrophys. J. Lett.* **883**, L42 (2019), 1908.09084.
- [12] S. R. Taylor, J. R. Gair, and I. Mandel, *Phys. Rev. D* **85**, 023535 (2012), 1108.5161.
- [13] W. Del Pozzo, T. G. F. Li, and C. Messenger, *Phys. Rev. D* **95**, 043502 (2017), 1506.06590.
- [14] D. E. Holz and S. A. Hughes, *Astrophys. J.* **629**, 15 (2005), astro-ph/0504616.
- [15] W. Del Pozzo, *Phys. Rev. D* **86**, 043011 (2012), 1108.1317.
- [16] H.-Y. Chen, M. Fishbach, and D. E. Holz, *Nature* **562**, 545 (2018), 1712.06531.
- [17] B. Abbott et al. (LIGO Scientific, Virgo), ArXiv e-prints (2019), 1908.06060.
- [18] B. Abbott et al. (LIGO Scientific, Virgo), *Phys. Rev.*

- Lett. **119**, 161101 (2017), 1710.05832.
- [19] G. M. Harry (LIGO Scientific Collaboration), *Class. Quant. Grav.* **27**, 084006 (2010).
- [20] F. Acernese et al. (Virgo Collaboration), *Class. Quant. Grav.* **32**, 024001 (2015), 1408.3978.
- [21] B. Abbott et al. (LIGO Scientific, Virgo, Fermi GBM, INTEGRAL, IceCube, AstroSat Cadmium Zinc Telluride Imager Team, IPN, Insight-Hxmt, ANTARES, Swift, AGILE Team, 1M2H Team, Dark Energy Camera GW-EM, DES, DLT40, GRAWITA, Fermi-LAT, ATCA, ASKAP, Las Cumbres Observatory Group, OzGrav, DWF (Deeper Wider Faster Program), AST3, CAASTRO, VINROUGE, MASTER, J-GEM, GROWTH, JAGWAR, CaltechNRAO, TTU-NRAO, NuSTAR, Pan-STARRS, MAXI Team, TZAC Consortium, KU, Nordic Optical Telescope, ePESSTO, GROND, Texas Tech University, SALT Group, TOROS, BOOTES, MWA, CALET, IKI-GW Follow-up, H.E.S.S., LOFAR, LWA, HAWC, Pierre Auger, ALMA, Euro VLBI Team, Pi of Sky, Chandra Team at McGill University, DFN, ATLAS Telescopes, High Time Resolution Universe Survey, RIMAS, RATIR, SKA South Africa/MeerKAT), *Astrophys. J. Lett.* **848**, L12 (2017), 1710.05833.
- [22] B. Abbott et al. (LIGO Scientific, Virgo, 1M2H, Dark Energy Camera GW-E, DES, DLT40, Las Cumbres Observatory, VINROUGE, MASTER), *Nature* **551**, 85 (2017), 1710.05835.
- [23] M. Soares-Santos et al. (DES, LIGO Scientific, Virgo), *Astrophys. J. Lett.* **876**, L7 (2019), 1901.01540.
- [24] M. Graham et al., *Phys. Rev. Lett.* **124**, 251102 (2020), 2006.14122.
- [25] LIGO Scientific Collaboration, Virgo Collaboration, Gamma-ray Coordinates Network **24621** (2017), URL <https://gcn.gsfc.nasa.gov/gcn3/24621.gcn3>.
- [26] R. Abbott et al. (LIGO Scientific, Virgo), *Phys. Rev. Lett.* **125**, 101102 (2020), 2009.01075.
- [27] R. Abbott et al. (LIGO Scientific, Virgo), *Astrophys. J. Lett.* **900**, L13 (2020), 2009.01190.
- [28] G. Ashton, K. Ackley, I. Magaña Hernández, and B. Piotrkowski, arXiv e-prints arXiv:2009.12346 (2020), 2009.12346.
- [29] B. McKernan, K. Ford, I. Bartos, M. Graham, W. Lyra, S. Marka, Z. Marka, N. Ross, D. Stern, and Y. Yang, *Astrophys. J. Lett.* **884**, L50 (2019), 1907.03746.
- [30] B. Sathyaprakash, B. Schutz, and C. Van Den Broeck, *Class. Quant. Grav.* **27**, 215006 (2010), 0906.4151.
- [31] S. R. Taylor and J. R. Gair, *Phys. Rev. D* **86**, 023502 (2012), 1204.6739.
- [32] S.-J. Jin, D.-Z. He, Y. Xu, J.-F. Zhang, and X. Zhang, *JCAP* **03**, 051 (2020), 2001.05393.
- [33] LIGO Scientific Collaboration and Virgo Collaboration, *GW190521 parameter estimation samples and figure data* (2020), URL <https://dcc.ligo.org/LIGO-P2000158/public>.
- [34] M. Isi, *GW190521: posterior samples conditional on AGN J1249+3449* (2020), URL <https://doi.org/10.5281/zenodo.4057131>.
- [35] P. Madau and M. Dickinson, *Ann. Rev. Astron. Astrophys.* **52**, 415 (2014), 1403.0007.
- [36] R. Abbott et al. (LIGO Scientific, Virgo), ArXiv e-prints (2019), 1912.11716.
- [37] V. Varma, S. E. Field, M. A. Scheel, J. Blackman, D. Gerosa, L. C. Stein, L. E. Kidder, and H. P. Pfeiffer, *Phys. Rev. Research* **1**, 033015 (2019), 1905.09300.
- [38] M. Fishbach et al. (LIGO Scientific, Virgo), *Astrophys. J. Lett.* **871**, L13 (2019), 1807.05667.
- [39] R. Gray et al., *Phys. Rev. D* **101**, 122001 (2020), 1908.06050.
- [40] T. J. Loredo, *AIP Conf. Proc.* **735**, 195 (2004), astro-ph/0409387.
- [41] I. Mandel, W. M. Farr, and J. R. Gair, *Mon. Not. Roy. Astron. Soc.* **486**, 1086 (2019), 1809.02063.
- [42] S. Vitale, ArXiv e-prints (2020), 2007.05579.
- [43] W. M. Farr and J. R. Gair, *A derivation of the likelihood function for a statistical h_0 measurement*, <https://github.com/farr/HOStatisticalLikelihood> (2020).
- [44] W. M. Farr, *Gw190521sky*, <https://github.com/farr/GW190521Sky> (2020).
- [45] W. Hu and S. Dodelson, *Ann. Rev. Astron. Astrophys.* **40**, 171 (2002), astro-ph/0110414.
- [46] S. Khan, F. Ohme, K. Chatziioannou, and M. Hannam, *Phys. Rev. D* **101**, 024056 (2020), 1911.06050.
- [47] S. Ossokine et al., *Phys. Rev. D* **102**, 044055 (2020), 2004.09442.
- [48] S. Mukherjee et al. (2020), in prep.
- [49] V. Gayathri et al. (2020), in prep.
- [50] B. Abbott et al. (KAGRA, LIGO Scientific, VIRGO), *Living Rev. Rel.* **21**, 3 (2018), 1304.0670.
- [51] T. Oliphant, *NumPy: A guide to NumPy*, USA: Trelgol Publishing (2006–), URL <http://www.numpy.org/>.
- [52] C. R. Harris et al., *Nature* **585**, 357 (2020), URL <https://doi.org/10.1038/s41586-020-2649-2>.
- [53] P. Virtanen et al., *Nature Meth.* **17**, 261 (2020), 1907.10121.
- [54] J. D. Hunter, *Comput. Sci. Eng.* **9**, 90 (2007).
- [55] D. Foreman-Mackey, D. W. Hogg, D. Lang, and J. Goodman, *Publ. Astron. Soc. Pac.* **125**, 306 (2013), 1202.3665.
- [56] The pandas development team, *pandas-dev/pandas: Pandas* (2020), URL <https://doi.org/10.5281/zenodo.3509134>.
- [57] Wes McKinney, in *Proceedings of the 9th Python in Science Conference*, edited by Stéfan van der Walt and Jarrod Millman (2010), pp. 56 – 61.
- [58] J. Salvatier, T. V. Wiecki, and C. Fonnesbeck, *PeerJ Computer Science* **2**, e55 (2016), 1507.08050.
- [59] M. Waskom et al., *mwaskom/seaborn: v0.10.1 (april 2020)* (2020), URL <https://doi.org/10.5281/zenodo.3767070>.
- [60] T. P. Robitaille et al. (Astropy Collaboration), *Astron. Astrophys.* **558**, A33 (2013), 1307.6212.
- [61] A. Price-Whelan et al., *Astron. J.* **156**, 123 (2018), 1801.02634.
- [62] H.-Y. Chen, C.-J. Haster, S. Vitale, W. M. Farr, and M. Isi, *Data release - A Standard Siren Cosmological Measurement from the Potential GW190521 Electromagnetic Counterpart ZTF19abnrhr* (2020), URL <https://doi.org/10.5281/zenodo.4057311>.